2024 IEEE International Conference on Robotics and Automation (ICRA 2024)
May 13-17, 2024. Yokohama, Japan

Real-time Dexterous Prosthesis Hand Control by Decoding Neural Information Based on EMG Decomposition

Zhenzhi. Ying, Xianyu. Zhang, Shihao. Li, Koki. Nakashima, Liming. Shu, Member, IEEE and Naohiko. Sugita

Abstract— **The vague interpretation of myoelectrical signals on the residual limb end makes restoring dexterous hand function in amputees still impossible. Understanding motor control between human motion intention and synaptic inputs to motor neurons also remains a significant challenge. The neural decoding methods of surface EMG signals remains challenging, which limit the application of robot hand in real life. Herein, we propose and substantiate a human-machine interface for motor control that introduces neural information of motor neurons in conjunction with the combination mechanism of muscle contraction. The interface firstly introduces a new concept of motor unit (MU) spike trains, which combines decoupling of the electrical activations on motor neuron axons with extraction of motion patterns from the discharge timings of the motor neuron pools. We realized a real-time implementation of the EMG decomposition algorithm on our developed prosthesis hand control system. The control scheme provides an accurate classification of intuitive hand motions, enabling the amputee to perform versatile finger movements of the prosthesis hand. The concept of motor neuron discharge timings was evaluated through experiments on one amputee participant and six able-bodied participants. The results show that the neuroprosthesis hand control scheme based on MU spike trains has the capacity of generating accurate and intuitive hand movements for amputees in a physical environment.**

I. Introduction

A human-machine interface satisfies the desire to intuitively control the prosthesis hand and restore the missing hand functions for upper limb amputees [1–5]. The electromyography (EMG) signals, that record the electrical signals generated during muscle contraction, are currently the only viable non-invasive human-machine interaction for controlling an externally powered prosthesis hand [6–10]. However, it is difficult to elucidate EMG because it is the sum of the action potentials of motor units (MUs) and noise [11]. Although commercially available and academic prosthesis hands that can drive five fingers independently have been developed [12–16], it is still challenging to estimate amputee's motion intention from EMG signals, this is because intrinsic muscles responsible for finger movements are thin and mostly located in deep layers of forearm muscle groups compared with that of the limb [17, 18]. The existing approaches based on machine learning have limited number of motion classifications and simultaneous control is not possible to ensure accuracy [19, 20]. Regression-based approaches allow simultaneous and proportional control but suffer from low precision and flexibility [21, 22]. Thus, a human-machine interface that satisfies high-precision and proportional prosthesis hand control has not yet been realized [23–25].

The EMG signals are constructed using motor neuron spike trains convolved with MU action potentials. The MU, which is composed of a motor neuron and all the muscle fibers innervated by the motor neuron, is the functional unit of the human motor control system and can control the force of a muscle contraction to coordinate muscle movements [26, 27]. Therefore, extracting the MU spike train from the EMG signal can help understand the neural information of the human motor intention during movement generation. Some previous research proposed EMG decomposition methods that enable the discrimination of individual MU action potential from multi-channel EMG signals [28, 29].

However, there are still deficiencies of current EMG decomposition methods due to the computation complexity of the algorithm. Most of these studies have focused on isometric contraction experiments and offline evaluations [27, 30, 31]. The analysis and utilization of MU spike train are also limited to brief superposition to obtain cumulative MU spike trains. Therefore, it is still challenging to apply the real-time EMG decomposition method to continuous dynamic movements and prosthesis control that is computationally complex, making the application in actual scenery impossible [32]. Moreover, there are currently no examples of upper-limb motor control neural information extraction and prosthesis hand manipulation based on online EMG decomposition.

Here, we propose a human-machine interface that extracts the motor neuron discharge timings from the surface EMG signals. Furthermore, the motion patterns are reconstructed with MU spike trains, thereby mapping them into human functional activities to recognize the motion intention. We experimentally validated the proposed motion recognition approach in the experiments of ten participants. Moreover, we developed a prosthesis hand with real-time implementation of the EMG decomposition algorithm for an amputee participant. With this new principle and the developed prosthesis hand control system, the extracted MU spike trains can be used to restore dexterous hand functions.

II. Methods

Fig. 1 shows the neural pathway for motor control and signal processing steps in our developed prosthesis hand

*Resrach supported by Japan Society for the Promotion of Science grant 23KJ0507 and the Central Universities, Dalian University of Technology, DUT22RC(3)064.

Zhenzhi. Ying, Xianyu. Zhang, Shihao. Li, Koki. Nakashima, and Naohiko. Sugita are with the Manufacturing Laboratory, Department of Mechanical Engineering, The University of Tokyo, Tokyo, 1138656 Japan (corresponding author to provide phone: +81-3-5841-6336; e-mail: sugi@mfg.t.u-tokyo.ac.jp).

Liming. Shu is with the Department of Mechanical Engineering, Dalian University of Technology, Dalian, 116024 China (corresponding author, e-mail: l.shu@dlut.edu.cn).

control system. First, the measured multichannel EMG signals were filtered and decoded to extract the discharge timings of the activated MUs (spike trains) from the muscle fiber action potentials using the EMG decomposition algorithm. Second, the firing rates of all motor neurons were calculated and used to estimate the extent of MU activation based on the LSTM network, thereby allowing for the determination of motion patterns. Subsequently, the actuators of the prosthesis hand were driven by the pulse width modulation (PWM) control command according to the recognized pattern result. The amputee can realize flexible motor control of digit movements using the developed real-time MU spike train-driven myoelectric prosthesis hand system.

A. EMG recording and processing

In the EMG signal measuring, the sampling frequency was unified to 2000Hz. In addition, the obtained data were rectified and then filtered by a bandpass filter of 5 to 250 Hz and notch filters of 50, 100, 150 and 200 Hz. Without loss of generality, we assumed that the observed variable (EMG signal) and the independent component (MU action potential) have zero means. In the preprocessing for EMG signal decomposition, data extension and whitening were performed [33]. The data extension is to extend the EMG data for the MU action potential generation time. First, in data extension, the EMG signals can be extended as follow by adding R delays for each observation:

$$\tilde{x}_i(n)=\left[x_i(n),x_i(n-1),\cdots,x_i(n-R)\right] \tag{1}$$

where n is discrete time and x_i is the EMG signal of i th channel.

Furthermore, whitening was also performed for signal decorrelation. Whitening makes each component uncorrelated, i.e., has a covariance of 0 and a variance of 1, and gives the orthogonal transformation of the independent components. In other words, the covariance and correlation matrices of the whitened vectors become identity matrices. The whitening of the extended data is calculated as follows, with W being the whitening matrix:

$$z(n)=W\tilde{x}(n) \tag{2}$$

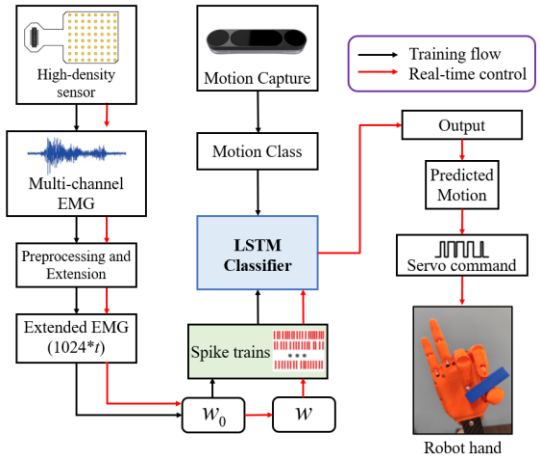

Figure 1. The pathway of the EMG processing and decoding procedure for training and robot hand control.

The whitening matrix W is obtained as follows:

$$W=D^{\gamma}U^{T} \tag{3}$$

where $\gamma=-1/2$. U is the diagonalization matrix of the covariance matrix of $\tilde{x}$, which is obtained by eigenvalue decomposition as follow:

$$R_{\tilde{x}\tilde{x}}=UDU^{T} \text{ with } R_{\tilde{x}\tilde{x}}=E\left(\tilde{x}(n)\tilde{x}^{T}(n)\right) \tag{4}$$

B. Neural Information Extraction

As mentioned in the result part, the original EMG signals are estimated as having independent components and non-Gaussian properties as follow:

$$\tilde{x}(n)=\sum_{l=0}^{L-1}H(l)\tilde{s}(n-l)+N(n) \tag{5}$$

where H is the action potential of MUs, $\tilde{s}$ is the MU spike train and N is the noise.

We used FastICA algorithm [34] to estimate the original independent components based on the fixed point algorithm that searches for the vector w to maximize the non-Gaussianity of the projection $w^{T}x$ of the observed signal x. Considering that the covariance matrix of $w^{T}x$ is the unit matrix:

$$E\left(\left(w^{T}x\right)^{2}\right)=\sum_{i,j}w_iw_jE\left(x_ix_j\right)=\|w\|^{2}=1 \tag{6}$$

since it is constrained that w is a unit vector, we consider the constraint that vector w is normalized to have a magnitude of 1. To derive the fixed point algorithm by the approximate Newton method, we used the Lagrangian method of undetermined multipliers to update the w as follow:

$$w(k)=E\left(xg\left(w(k-1)^{T}x\right)\right)-E\left(g'\left(w(k-1)^{T}x\right)\right)w(k-1) \tag{7}$$

where k is the number of iterations and g is the derivative of a general contrast function that measures the sparseness. By performing further normalization and iterating this until w converges, we can search for one w that maximizes the non-Gaussianity of the projection $w^{T}x$. All components can be searched by repeating this for a new w each time it converges and orthogonalizing the ws each time. This process is repeated N times for the preset number of MUs to be extracted. Thus, the orthogonal transformation matrix (separation matrix) is finally obtained.

Using the vector w obtained in the above process, the action potential of the j th MU at discrete time n is estimated as follows:

$$\tilde{s}_j(n)=w_j^{T}x(n) \tag{8}$$

Further, this signal is squared to detect its peak, which is a MU spike train. At this time, the squared signal is binarized by the K-means algorithm, which is the clustering algorithm to detect spikes.

In order to verify whether the MU spike train obtained by the K-means algorithm is valid, we perform an evaluation based on SIL analysis. This is based on the SIL distance, which is refined for each signal and ranges from -1 to +1. If this value is large, the point is far enough away from other clusters, that is, the clustering is reasonable. This process is calculated for each extracted MU, and only when the SIL exceeds the threshold (0.9 in this study), it is adopted as a valid MU spike train. Therefore, in many cases, the number of MUs actually employed is smaller than the preset N .

C. Motion Recognition

After extracting the motor neuron discharging times, we calculated the firing rate of each MU as the features of motion recognition. The firing rate matrix was then input to a recurrent neural network classifier to perform discrete classification of motion intentions. The firing rate F per unit time for j th MU were calculated as follow:

$$F_j(n) = \frac{st_j(n)}{L} \tag{9}$$

where L is the sample length, ST is the number of spikes fired per unit time.

To construct the motion pattern with the decomposed EMG signals, we exploited long short-term memory (LSTM) network to extract the motion patterns from the MU spike trains. The architecture of the proposed LSTM model that estimated the motion classification was depicted in Fig. 2. The calculated MU firing rates were transferred to LSTM network layers, and then went through fully connected layer. In our study, the time window was set to be 200ms, and the number of hidden units in the LSTM network were selected as 16. The dropout probability of LSTM layers was set to 0.2. The time steps for training LSTM model is 10. The Batch size was 128 and epoch was set as 100.

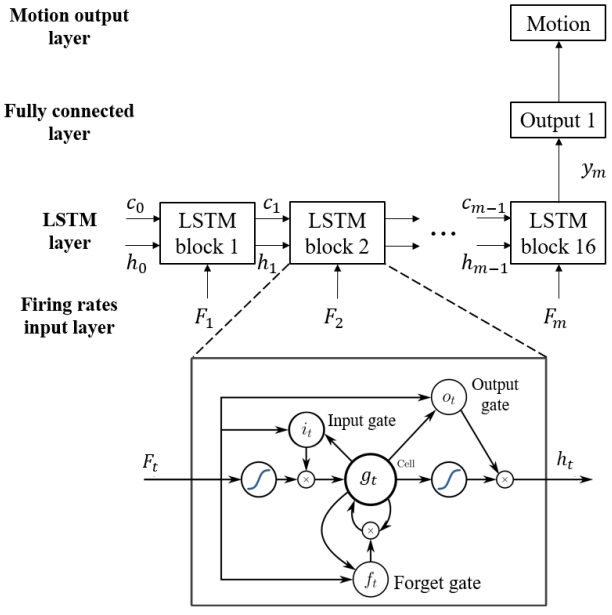

Figure 2. The architecture of the proposed LSTM-based motion classifer.

C. Real-time Implementation

The use of the human-machine interface based on our proposed EMG decomposition needs to be carried out online to control the actuators of the prosthesis hand to achieve intuitive motions in the closed-loop user scenario. We proposed a real-time update strategy for the EMG decomposition processing to reduce computation complexity. The separation vector and the cluster centers from the training process were reserved for use in the real-time spike train extraction. Rather than a random initial weight vector, the reserved separation vector was used directly in the algorithm, which greatly reduced the number of iterations (from >100 iterations to < 3 iterations). In this process, we aim to maximize the evaluation function using Lagrangian method as follow:

$$L = E\left(G\left(w_0{}^T x\right)\right) + \beta\left(\|w_0\|^2 - 1\right) \tag{10}$$

where w_0 is the saved w in the training process, and the maximum happens when the gradient approaches to 0:

$$\frac{\partial L}{\partial w} = E\left(xg\left(w^T x\right)\right) + \beta w = 0 \tag{11}$$

The cluster centers for the real-time incoming MU spike trains were updated as follow:

$$T(n) = \frac{c_1 T(n-1) + c_2 T}{c_1 + c_2} \tag{12}$$

where c_1 is the number of identified spikes in the last package MU spike train and c_2 is set as 10 empirically.

The developed prosthesis hand control system consisted of the prosthesis hand, control circuit, power supply and socket. The main body of the prosthesis hand was 3D-printed from NinjaFlex filament (1.75mm, NinjaTek Ltd.,), whose material properties are close to the human muscle (shore hardness, 85A). We modified the open-source hand model Ada Robotic Hand (Open Bionics) to print the palm parts. The prosthesis hand is soft and flexible with high stretchy to not inhibit mobility as shown in Fig. 3(A). The fingertips of the prosthesis hand were pulled by linear actuators (PQ12-P, Actuonix Ltd.,) through strings to allow flexion/extension movements of two finger joints. The various finger motions were controlled by pulse-width modulation from a control circuit (Arduino Mega 2560, L293D module) through serial communication to the LSTM-based classifier python script.

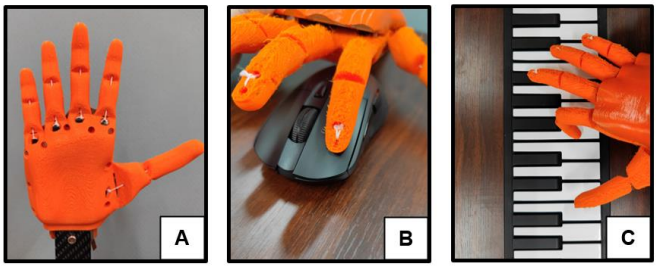

Figure 3. Photographs of (A) the developed prosthesis hand and interacting with the environment such as (B) mouse clicking and (C) piano playing.

III. Results

Experiments were performed on one upper-limb amputee participant and six able-bodied participants to validate the effectiveness of our developed real-time spike train-based prosthesis control system. In Experiment 1, able-bodied and amputee participants performed numerous hand motions using our proposed EMG decomposition-based motion recognition to compare the classification results. In Experiment 2, we developed a prosthesis control system, and the amputee participant controlled the prosthesis to restore dexterous hand functions using the extracted MU spike trains.

A. Experimental Protocol

High-density EMG sensor (GR10MM0808, OT Bioelettronica Ltd.,) was used to record multi-channel EMG signals, which is a 64-channel (8x8) myoelectric electrode grid, with a distance of 10 mm between each electrode. With respect to an amplifier for EMG data, we used an RHD 1024ch recording controller (Intan Technologies Ltd.,) that can measure biological signal data of up to 1024 channels. In addition, we designed and manufactured connection boards to connect the amplifier and the high-density myoelectric sensors which allowed EMG signals on the sensors to be mapped to the corresponding amplifier channels. The hand and finger movements were recorded using an optical hand motion tracking system (Leap Motion, Ultrahaptics Ltd.,) with a sampling frequency of 100Hz.

One amputee and six able-bodied participants were voluntarily recruited in the experiments. They were informed of the purpose and details of the research beforehand with the consent of a rehabilitation doctor. All the experiments were designed by following the relevant legislation based on the Engineering Ethics Committee's Human Experiment Implementation Regulations of the University of Tokyo (approval no. KE14-72) and in compliance with the Declaration of Helsinki.

In all the experiments, two high-density myoelectric sensors were attached to the forearm so as to cover the muscles in the anterior and posterior compartments of the forearm. One sheet was attached on the palmar side of the hand parallel to the ulnar side, at a position approximately 5 cm from the olecranon, and the EMG signals of the FD superficialis, FD profundus, and flexor pollicis longus were measured. The other one was placed on the dorsal side of the hand, mainly on the radialis side to measure the EMG signals from the ED communis and extensor pollicis longus. Each of these data will be referred to as flexor and extensor data in the results. After attaching the high-density myoelectric sensor using conductive cream (CC1, OT Bioelettronica Ltd.,), it was fixed by medical taping to prevent the sensor from slipping.

The amputee participant is unilateral transradial amputee, and thus he attempted to conduct mirror motions of the missing and contralateral upper limb to ensure the intuitive motion intentions. The motion intentions to the participant's CNS in each 128ms interval were estimated by extracting MU spike trains from the multi-channel EMG signals. The motion capture and EMG signals were measured synchronously. Classification accuracy was defined as the error between the classification result and actual motion estimated by the recorded finger joint angles. The global time-frequency EMG features (RMS values) were also extracted to classify the motion intention with the same classifier and time interval for comparison.

B. Experiment 1: Neural information decoding

The aim of this experiment is to establish whether it is possible to estimate motion intention accurately based on our proposed EMG decomposition algorithm. All participants (one amputee and six able-bodied participants) participated in experiment 1. In this experiment, the participants were asked to perform the following hand motions: thumb flexion/extension, index finger flexion/extension, middle finger flexion/extension, ring finger flexion/extension, little finger flexion/extension, two finger (thumb-index) grasp, three finger (thumb-index/middle) grasp, five finger grasp. All participants sat with their elbows on the table and their upper arms extended naturally. With their palms up, they followed the prompts on the computer screen to perform the specified motions in succession. In each trial, the participant performed every motion three times with 3-second rest. The participant repeated the trials 10 times and took 5 minutes of rest between trials to avoid muscle fatigue. All collected trial data were divided into training data and test data in the proportion of 80/20%. The training data were used to confirm the motion classifier for extracted MU spike trains.

Fig. 4(A) shows the 128-channel EMG signals that were measured when the participants performed five single-finger motions. Fig. 4(B) shows the decomposed MU spike trains from the recorded EMG data, where one vertical bar in one row represents that distinct motor neurons of this MU discharg at the time sampling point. Most motor neurons exhibited discharges in the index and little finger movements in either amputee or able-bodied participants. Fig. 5(A) shows the confusion matrices of the nine classification results (eight tested motions and relaxed state) for all the amputee and able-bodied participants. The average accuracy of the motion classification is excellent using MU spike train from the motor neuron discharging time for amputee (accuracy of 92.7%) and able-bodied participants (average accuracy of 96.4%), as shown in Fig. 5.

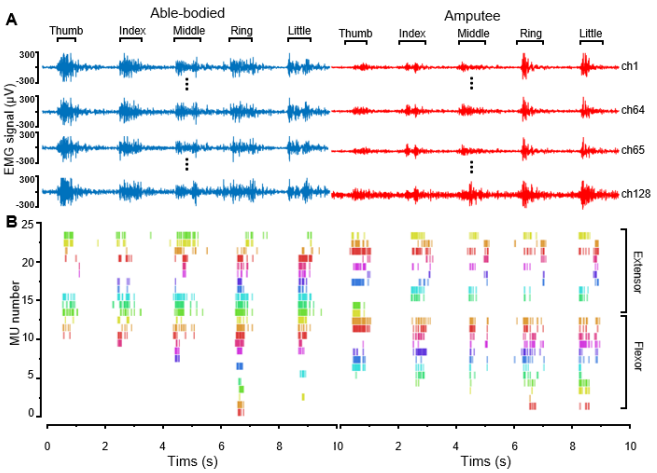

Figure 4. (A) All multi-channel EMG signals from the flexor and extensor forearm muscle groups of able-bodied and amputee participants. (B) Extracted MU spike trains from EMG signals for each finger movements.

We observed that amputee participants had trouble controlling the middle, ring, and little finger movements, resulting in an inferior classification result among the three grasp hand motions. For comparison, the classification using time-varying EMG feature root mean square (RMS) was also performed using the same experimental data. To statistically consider the classification results for the EMG decomposition-based method and the RMS-based method, t-tests were performed to compare the difference ($P < 0.05$). The null hypothesis was rejected, and a significant difference was suggested. The statistical analyses further demonstrate that the proposed MU spike train motion recognition algorithm was significantly superior to using this classical global EMG spatial-temporal features, which is valid for all amputee and able-bodied participants. The classification results and corresponding prosthesis hand operations for the eight tested motions are shown in the accompanying video.

Compared to the global EMG amplitude, the activation of the intrinsic MU responsible for a single finger is much more discriminable in MUS activation. This experiment demonstrates that the use of motor neuron discharging time and LSTM-based classifier is beneficial for extracting the true motor intention of the amputee on the missing limb using non-invasive HD-EMG signals.

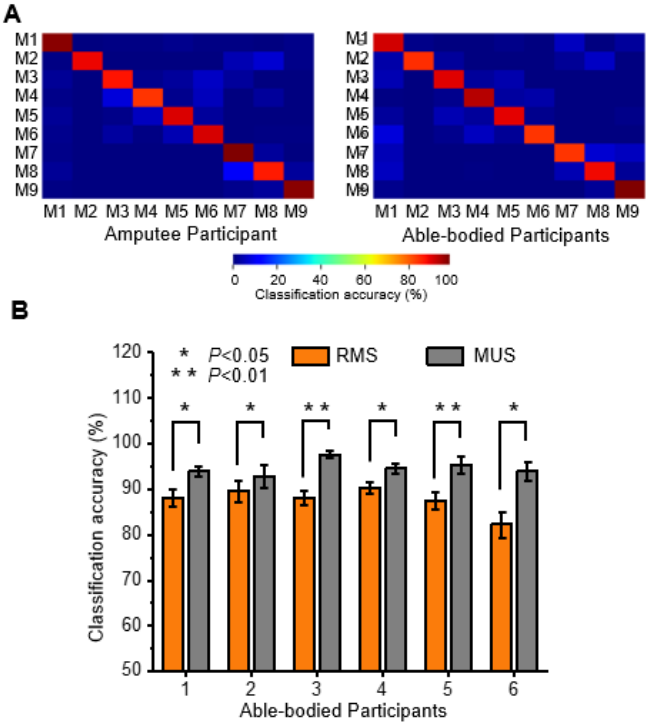

Figure 5. Experimental results for motion classification. (A) Confusion matrices for the hand motion classifications among all participants. The horizontal axis represents the true motion and vertical axis represents the identified motions. (The hand motions are: rest (M1), thumb, index, middle, ring and little finger flextion/extension (M2 - M6), two, three and five finger grasp (M7 – M9). (B) Average classification accuracies for all the hand motion classifications among all able-bodied participants when using extracted MU spike trains and when using extracted global EMG RMS.

C. *Experiment 2: Real-time prosthesis control in a physical environment*

Experiment 2 was performed on an amputee participant with the purpose of testing the performance of the developed prosthesis hand system using the extracted neural information. The amputee participant sat in front of a table and wear a specially designed socket that connected the residual limb and prosthesis hand. The EMG sensors were located on the anterior and posterior of the residual forearm. In the experiment, the participant was asked to attempt the following two hand function tasks: mouse clicking and piano playing. These hand function tasks are combinatorial variants of the motions in Experiment 1 and are also considered to be widely used in amputee's physical and spiritual life. In addition, the participant did not perform the mirror movement in these tasks to better restore the application in daily life.

At first, the amputee participant's recorded EMG data in experiment 1 was used to extract the separate matrix and cluster centers for real-time control. The participant was then asked to perform the evaluation task and races of the proposed hand function tasks.

During the evaluation trail of the mouse clicking task, the participant was asked to alternate left and right click on the mouse for 10 times. To realize the successful mouse clicking, the participant was instructed to place the palm of the prosthesis hand against the bottom of the mouse to prevent slippage. The valid mouse clicking was identified by a web mouse applet. We counted the interval time between two valid clicks to evaluate the accuracy and timeliness of the index and middle finger flexion/extension motions using our MU spike train principle. In the evaluation trial of the piano playing test, the participant was asked to attempt five single-finger motions 100 times to complete piano key pressing. In addition, we asked the participant to use different fingers to press a key one key (or three, five keys) away from the last press freely to simulate the real scene of playing the piano. The amputee participant took a 5-minute break between each trial and a 20-minute rest between each task.

The evaluation results for the hand function tasks are shown in Fig. 6. Fig. 6(A) shows the percentage of successful trials for the evaluation tests of three hand function tasks. With the MU spike train-based control system, the amputee participant achieved considerably higher successful rates for the two hand function tasks. During the mouse-click task, the amputee participant performed left and right clicks while freely switching from index finger motion to middle finger motion. A successful mouse click trial is defined as an intact index or middle finger flexion/extension movement with an appropriate pressing of the mouse button. In addition to the successful rate, we assessed the completion time for one click as shown in Fig. 6(B). Furthermore, we demonstrated that the amputee participant can intuitively control a single prosthesis finger to press the keys of the piano to play a song, similar to an able-bodied pianist. This task aims to evaluate the potential of MU spike train-based control in decoding human-motion intention and intuitive human–machine interaction. In this task, the amputee tried to think about putting the finger on the correct piano key rather than intending to flex the finger and move the hand. In the evaluation test, we asked the amputee participant to move the prosthesis hand to press the keys at a

certain distance (one, three, and five keys) after finishing the last key pressing as shown in Fig. 6(C). In addition, it can be observed that the participant has little difficulty in controlling specific MU groups associated with the middle, ring, and little fingers, consistent with the results of Experiment 1. Importantly, the amputee was capable of playing the piano by delicately controlling the single-finger flexion/extension.

The results in Fig. 6 demonstrate superior performance with MU spike train-based control in terms of the two metrics. On the basis of the statistical analyses, EMG activity is significantly different for MU spike train-based and RMS-based control ($P<0.05$, Fisher's exact test). Wilcoxon signed-rank test was also used to show statistical significance in the case of interval time between effective mouse-clicking ($P<0.05$). When considered together, these results illustrate that the MU spike train-based prosthesis hand control system can aid in more accurate finger movement, flexible motion transition, and avoid accidental misoperations.

IV. Disscussion

Here, we demonstrated that we are capable of decoding the motor neuron discharge information and restoring motion intention. In addition, the realization of a real-time prosthetic hand control system for dexterous finger movements is presented.

In Experiment 1, the MU spike trains were extracted from the EMG signals and combined to represent different motions. All test motions were recognized based on EMG decomposition and MU spike train classification with a higher accuracy compared to the EMG temporal feature-based classification. Fig. 4(B) highlights the reason for the superior motion recognition using the MU spike train-based classification algorithm. The decomposition of the EMG signal filters out surface myoelectrical changes (non-Gaussian noise) and reserves the activation of detailed muscle fibers, rather than the integral muscle activation level. Among the forearm muscle groups, the muscle fibers related to single-finger motions are interdigitated and overlapped spatially, especially index, middle, ring, and little fingers share FD and extensor digitorum (ED). To recognize different motions, the combinations of MU spike train can eliminate the influence of muscle overlap and provide a conversely clear mapping of the contribution of muscles. The spatial distribution results are partly in agreement with that reported in previous studies. [22] Their results found the neural inputs to the motor neurons of FD superficialis are grouped into two different forms. Several previous studies examining neural inputs to other MU pools also support our claim that the synaptic inputs to functional motion patterns may include different MU pools, such as between ED communis and FD superficialis, and between FD profundus and flexor pollicis longus [35, 36]. Our proposed human-machine interface allowed flexibility of number and composition in motor neuron recruitment for the MU grouping to accommodate various hand functions.

This study currently is the first real-time implementation of EMG decomposition in the human-machine interface, which overcomes the difficulties of computational complexity and dynamic environment diversification for a user in a practical scenario. As of now, the clinical performance of our

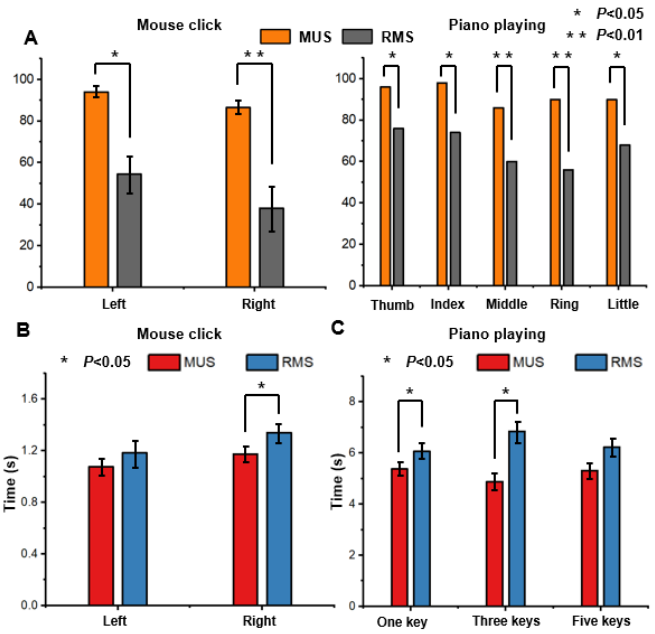

Figure 6. (A) The successful rates of three tasks in the evaluation tests (Fisher's exact test). (B) The interval times between two valid mouse clicks in the evaluation tests of mouse clicking task (Wilcoxon two-sided signed-rank test). (C) The interval times between two valid piano pressings across one, three and five keys in the evaluation tests of piano playing task (Fisher's exact test).

proposed MU spike train-based control scheme depends on the efficacy of the prosthesis hand mechatronics design; for example, in the prosthesis hand, the agility of finger movements is always in conflict with the weight load of the actuators. Therefore, future studies should include dexterous robot hands equipped with high-torque motors and sensory sensors, which would significantly benefit closed-loop intuitive control implementation. The robustness of MU grouping principles for different motion patterns or mechanical constraints and recruitment order based on MU spike train are also required to be investigated further.

V. Conclusion

In conclusion, we proposed a human–machine interface to decode the discharge timings of MUs to the reconstructed spike train input representing the human motor intention from the central nervous system. This interface was demonstrated through valid experiments with seven participants, and the possibility of providing credible and intuitive control commands to the prosthesis hand was proved. The proposed MU spike train principle is an ultimate exploration of the human neural motor control that combines macroscopic motion dimensionality reduction and microscopic analysis (intercellular interactions of motor neurons). We realized real-time implementation of the proposed MU spike train principle to reproduce complex hand functions on the prosthesis hand.

REFERENCES

[1] D. Farina, O. Aszmann, Bionic limbs: Clinical reality and academic promises. Sci. Transl. Med. 6, 6–10 (2014).

[2] L. Zollo, G. Di Pino, A. L. Ciancio, F. Ranieri, F. Cordella, C. Gentile, E. Noce, R. A. Romeo, A. D. Bellingegni, G. Vadalà, S. Miccinilli, A. Mioli, L. Diaz-Balzani, M. Bravi, K. P. Hoffmann, A. Schneider, L. Denaro, A. Davalli, E. Gruppioni, R. Sacchetti, S. Castellano, V. Di Lazzaro, S. Sterzi, V. Denaro, E. Guglielmelli, Restoring tactile sensations via neural interfaces for real-time force-and-slippage closed-loop control of bionic hands. Sci. Robot. 4, 1–12 (2019).

[3] D. W. Tan, M. A. Schiefer, M. W. Keith, J. R. Anderson, J. Tyler, D. J. Tyler, A neural interface provides long-term stable natural touch perception. Sci. Transl. Med. 6, 1–12 (2014).

[4] J. A. George, D. T. Kluger, T. S. Davis, S. M. Wendelken, E. V. Okorokova, Q. He, C. C. Duncan, D. T. Hutchinson, Z. C. Thumser, D. T. Beckler, P. D. Marasco, S. J. Bensmaia, G. A. Clark, Biomimetic sensory feedback through peripheral nerve stimulation improves dexterous use of a bionic hand. Sci. Robot. 4, 1–12 (2019).

[5] E. D'Anna, G. Valle, A. Mazzoni, I. Strauss, F. Iberite, J. Patton, F. M. Petrini, S. Raspopovic, G. Granata, R. Di Iorio, M. Controzzi, C. Cipriani, T. Stieglitz, P. M. Rossini, S. Micera, A closed-loop hand prosthesis with simultaneous intraneural tactile and position feedback. Sci. Robot. 4 (2019), doi:10.1126/scirobotics.aau8892.

[6] J. Kang, D. Martelli, V. Vashista, I. Martinez-Hernandez, H. Kim, S. K. Agrawal, Robot-driven downward pelvic pull to improve crouch gait in children with cerebral palsy. Sci. Robot. 2, eaan2634 (2017).

[7] A. J. Young, L. H. Smith, E. J. Rouse, L. J. Hargrove, Classification of Simultaneous Movements Using Surface EMG Pattern Recognition. IEEE Trans. Biomed. Eng. 60, 1250–1258 (2013).

[8] D. Farina, I. Vujaklija, R. Brånemark, A. M. J. Bull, H. Dietl, B. Graimann, L. J. Hargrove, K. P. Hoffmann, H. (Helen) Huang, T. Ingvarsson, H. B. Janusson, K. Kristjánsson, T. Kuiken, S. Micera, T. Stieglitz, A. Sturma, D. Tyler, R. F. f. Weir, O. C. Aszmann, Toward higher-performance bionic limbs for wider clinical use. Nat. Biomed. Eng. (2021), doi:10.1038/s41551-021-00732-x.

[9] D. Farina, N. Jiang, H. Rehbaum, A. Holobar, B. Graimann, H. Dietl, O. C. Aszmann, The extraction of neural information from the surface EMG for the control of upper-limb prostheses: Emerging avenues and challenges. IEEE Trans. Neural Syst. Rehabil. Eng. 22, 797–809 (2014).

[10] G. Durandau, W. F. Rampeltshammer, H. Van Der Kooij, M. Sartori, Neuromechanical Model-Based Adaptive Control of Bilateral Ankle Exoskeletons: Biological Joint Torque and Electromyogram Reduction Across Walking Conditions. IEEE Trans. Robot. 38, 1380–1394 (2022).

[11] J. E. Cheesborough, L. H. Smith, T. A. Kuiken, G. A. Dumanian, Targeted muscle reinnervation and advanced prosthetic arms. Semin. Plast. Surg. 29, 62–72 (2015).

[12] P. D. Marasco, J. S. Hebert, J. W. Sensinger, D. T. Beckler, Z. C. Thumser, A. W. Shehata, H. E. Williams, K. R. Wilson, Neurorobotic fusion of prosthetic touch, kinesthesia, and movement in bionic upper limbs promotes intrinsic brain behaviors. Sci. Robot. 6 (2021), doi:10.1126/scirobotics.abf3368.

[13] J. T. Belter, J. L. Segil, A. M. Dollar, R. F. Weir, Mechanical design and performance specifications of anthropomorphic prosthetic hands: A review. J. Rehabil. Res. Dev. 50, 599–618 (2013).

[14] F. Cordella, A. L. Ciancio, R. Sacchetti, A. Davalli, A. G. Cutti, E. Guglielmelli, L. Zollo, Literature review on needs of upper limb prosthesis users. Front. Neurosci. 10, 1–14 (2016).

[15] M. Laffranchi, N. Boccardo, S. Traverso, L. Lombardi, M. Canepa, A. Lince, M. Semprini, J. A. Saglia, A. Naceri, R. Sacchetti, E. Gruppioni, L. De Michieli, The Hannes hand prosthesis replicates the key biological properties of the human hand. Sci. Robot. 5, 1–16 (2020).

[16] J. A. E. Hughes, P. Maiolino, F. Iida, An anthropomorphic soft skeleton hand exploiting conditional models for piano playing. Sci. Robot. 3, 1–13 (2018).

[17] F. V. G. Tenore, A. Ramos, A. Fahmy, S. Acharya, R. Etienne-Cummings, N. V Thakor, Decoding of Individuated Finger Movements Using Surface Electromyography. IEEE Trans. Biomed. Eng. 56, 1427–1434 (2009).

[18] J. G. Ngeo, T. Tamei, T. Shibata, Continuous and simultaneous estimation of finger kinematics using inputs from an EMG-to-muscle activation model. J. Neuroeng. Rehabil. 11, 122 (2014).

[19] G. Gu, N. Zhang, H. Xu, S. Lin, Y. Yu, G. Chai, L. Ge, H. Yang, Q. Shao, X. Sheng, X. Zhu, X. Zhao, A soft neuroprosthetic hand providing simultaneous myoelectric control and tactile feedback. Nat. Biomed. Eng. (2021), doi:10.1038/s41551-021-00767-0.

[20] K. Z. Zhuang, N. Sommer, V. Mendez, S. Aryan, E. Formento, E. D'Anna, F. Artoni, F. Petrini, G. Granata, G. Cannaviello, W. Raffoul, A. Billard, S. Micera, Shared human–robot proportional control of a dexterous myoelectric prosthesis. Nat. Mach. Intell. 1, 400–411 (2019).

[21] J. M. Hahne, M. A. Schweisfurth, M. Koppe, D. Farina, Simultaneous control of multiple functions of bionic hand prostheses: Performance and robustness in end users. Sci. Robot. 3 (2018), doi:10.1126/scirobotics.aat3630.

[22] M. Sartori, G. Durandau, S. Došen, D. Farina, Robust simultaneous myoelectric control of multiple degrees of freedom in wrist-hand prostheses by real-time neuromusculoskeletal modeling. J. Neural Eng. 15 (2018), doi:10.1088/1741-2552/aae26b.

[23] E. Biddiss, T. Chau, Upper-Limb Prosthetics: Critical Factors in Device Abandonment. Am. J. Phys. Med. Rehabil. 86 (2007)

[24] E. Biddiss, T. Chau, Upper limb prosthesis use and abandonment: A survey of the last 25 years. Prosthet. Orthot. Int. 31, 236–257 (2007).

[25] P. Geethanjali, Myoelectric control of prosthetic hands: State-of-the-art review. Med. Devices Evid. Res. 9, 247–255 (2016).

[26] D. Farina, A. Holobar, Characterization of Human Motor Units from Surface EMG Decomposition. Proc. IEEE. 104, 353–373 (2016).

[27] D. Farina, I. Vujaklija, M. Sartori, T. Kapelner, F. Negro, N. Jiang, K. Bergmeister, A. Andalib, J. Principe, O. C. Aszmann, Man/machine interface based on the discharge timings of spinal motor neurons after targeted muscle reinnervation. Nat. Biomed. Eng. 1 (2017), doi:10.1038/s41551-016-0025.

[28] C. Chen, Y. Yu, X. Sheng, X. Zhu, Non-Invasive Analysis of Motor Unit Activation During Simultaneous and Continuous Wrist Movements. IEEE J. Biomed. Heal. Informatics. 26, 2106–2115 (2022).

[29] C. Dai, X. Hu, Finger Joint Angle Estimation Based on Motoneuron Discharge Activities. IEEE J. Biomed. Heal. Informatics. 24, 760–767 (2020).

[30] M. Sartori, U. Yavuz, D. Farina, In Vivo Neuromechanics: Decoding Causal Motor Neuron Behavior with Resulting Musculoskeletal Function. Sci. Rep. 7, 1–14 (2017).

[31] C. Chen, Y. Yu, S. Ma, X. Sheng, C. Lin, D. Farina, X. Zhu, Hand gesture recognition based on motor unit spike trains decoded from high-density electromyography. Biomed. Signal Process. Control. 55, 101637 (2020).

[32] C. Chen, G. Chai, W. Guo, X. Sheng, D. Farina, X. Zhu, Prediction of finger kinematics from discharge timings of motor units: Implications for intuitive control of myoelectric prostheses. J. Neural Eng. 16 (2019), doi:10.1088/1741-2552/aaf4c3.

[33] F. Negro, S. Muceli, A. M. Castronovo, A. Holobar, D. Farina, Multi-channel intramuscular and surface EMG decomposition by convolutive blind source separation. J. Neural Eng. 13 (2016), doi:10.1088/1741-2560/13/2/026027.

[34] A. Hyvärinen, E. Oja, Independent component analysis: algorithms and applications. Neural Networks. 13, 411–430 (2000).

[35] F. D. Bremner, J. R. Baker, J. A. Stephens, Correlation between the discharges of motor units recorded from the same and from different finger muscles in man. J. Physiol. 432, 355–380 (1991).

[36] G. B. Hockensmith, S. Y. Lowell, A. J. Fuglevand, Common input across motor nuclei mediating precision grip in humans. J. Neurosci. 25, 4560–4564 (2005).